

# SEARCHES FOR R-PARITY VIOLATING SUPERSYMMETRY AT HERA

E. PEREZ

*CEN-Saclay, DSM/DAPNIA/SPP,  
Gif-sur-Yvette, France  
E-mail: eperez@frcpn11.in2p3.fr*

Y. SIROIS<sup>a</sup>

*LPNHE Ecole Polytechnique, IN2P3-CNRS,  
Palaiseau, France  
E-mail: sirois@polhp2.in2p3.fr*

The search for R-parity violating Supersymmetry at HERA is reviewed with emphasis on the resonant production of squarks through electron-quark fusion via lepton flavour violating Yukawa couplings  $\lambda'$ . The full consequences of the mixing in the gaugino-higgsino sector on the possible squark decay chains are taken into account and a rich phenomenology emerges for HERA. Direct searches carried recently by the HERA experiments show a sensitivity to yet unexplored domains of the squark mass- $\lambda'$  plane. The analysis of  $2.83 \text{ pb}^{-1}$  of  $e^+p$  data by H1 excludes squark masses up to 240 GeV for  $\lambda' \gtrsim \sqrt{4\pi\alpha_{em}}$  and covers with good discriminating power a wide range of parameters values in supersymmetric theories with minimal field representation. For squarks possessing  $\lambda'$  couplings to more than one generation of leptons, the analysis of  $3.8 \text{ pb}^{-1}$  of  $e^-p$  and  $e^+p$  data by the ZEUS experiment excludes masses up to 210 GeV for  $\lambda' \gtrsim \sqrt{4\pi\alpha_{em}}$  in models where the lightest gaugino-higgsino is a “pure” photino. The HERA results are compared in detail to other direct and indirect searches and future prospects are discussed.

## 1 Introduction

Supersymmetry (SUSY) which connects elementary fermions and bosons is generally considered to be a likely ingredient of a true fundamental theory beyond the Standard Model (SM). Traditionally, the study of observable consequences of SUSY at energy scales well below the SUSY breaking scale have been guided mostly by the theoretical framework of either the general Minimal Supersymmetric extension of the Standard Model (MSSM)<sup>1</sup> or of the more restrictive Supergravity<sup>2</sup>. Given a finite and well defined set of free parameters, both theories offer predictive power and have neither been proven nor falsified by experimental observations. In the strict MSSM framework, one imposes that the SUSY theory be minimal not only in field content but also in terms of allowed couplings. This is realized by imposing a strict conservation of the R-parity defined as  $R_p = (-1)^{3B+L+2S} = 1$  (for particles) =  $-1$  (for

---

<sup>a</sup>Invited speaker.

sparticles), where  $S$  denotes the spin,  $B$  the baryon number and  $L$  the lepton number. Imposing this discrete symmetry is a somewhat *ad hoc* prescription which leads to the absolute stability of the lightest supersymmetric particle (LSP). Hence to the characteristic hunt for “missing energy” signals in direct searches at other existing colliders. But Nature might, after all, choose an unstable LSP.

The essential instability of supersymmetric matter even seems very “natural” when considering that the general SUSY superpotential allows beyond the MSSM for gauge invariant terms with  $R_p$ -violating ( $\tilde{R}_p$ ) Yukawa couplings between the SM quarks and leptons and their bosonic squark ( $\tilde{q}$ ) or slepton ( $\tilde{l}$ ) partners. This will be discussed in section 2 where we briefly review and motivate the general  $\tilde{R}_p$  SUSY theory. Thus, the LSP becomes unstable through e.g. (virtual) conversion to fermion-sfermion pairs followed by sfermion decay via a Yukawa coupling. This has dramatic consequences. Besides the obvious fact that the LSP does not qualify anymore as a candidate for Cold Dark Matter in cosmology, it moreover invalidates many existing constraints on sparticle masses and other model parameters. The LSP decay leads to event topologies which differ strongly from the characteristic “missing energy” signal due to LSP’s escaping detection in the MSSM. Hence, except for exclusion limits derived from indirect searches (e.g. from the intrinsic width of the  $Z^0$ ), the mass constraints obtained in the MSSM framework do not apply directly in  $\tilde{R}_p$  models. The search for  $\tilde{R}_p$  squarks is “complementary” (hence mandatory) to that performed in the strict MSSM framework.

The  $ep$  collider HERA which provides both leptonic and baryonic quantum numbers in the initial state is found to be ideally suited for  $\tilde{R}_p$  SUSY searches. The rich phenomenology expected for Yukawa couplings which induce lepton number violating processes will be discussed in section 3. The direct constraints on such couplings imposed by recent analyses of H1 and ZEUS experiments at HERA and at other colliders are reviewed in section 4 and compared to results from indirect searches in section 5. The future discovery prospects at HERA are discussed in section 6. The main concepts and results are summarized in section 7.

## 2 The General Yukawa Couplings in SUSY

Preserving the minimal field content of the MSSM, the most general Yukawa couplings allowed by the SM requirement of  $SU(3)_C \times SU(2)_L \times U(1)_Y$  gauge invariance in a SUSY theory can be written<sup>3,4</sup> in the compact formalism of the superpotential as  $W_{SUSY} = W_{MSSM} + W_{\tilde{R}_p}$ . The  $W_{MSSM}$  contains terms which are responsible for the Yukawa couplings of the Higgs fields to ordinary

fermions. The additional  $W_{\mathcal{H}_p}$  terms<sup>b</sup> are given by:

$$W_{\mathcal{H}_p} = \lambda_{ijk} L_i L_j \bar{E}_k + \lambda'_{ijk} L_i Q_j \bar{D}_k + \lambda''_{ijk} \bar{U}_i \bar{D}_j \bar{D}_k \quad (1)$$

where  $ijk$  are generation indices of the superfields  $L, Q, E, D$  and  $U$ . The  $L$  and  $Q$  are left-handed doublets while  $\bar{E}, \bar{D}$  and  $\bar{U}$  are right-handed singlet superfields for charged leptons, down and up-type quarks, respectively. The  $\lambda$  and  $\lambda'$  terms induce  $I'$ . The  $\lambda''$  terms induce  $\mathcal{H}$ . The  $I'$  terms arise in a fundamental way from the fact that  $SU(2)$ -doublet lepton superfields and the Higgs  $H_1$  superfield are identical when viewed from the SM gauge symmetry. The  $\lambda_{ijk}$  ( $\lambda''_{ijk}$ ) couplings are antisymmetric under the interchange of the first (last) two generation indices,  $\lambda_{ijk} = -\lambda_{jik}$  and  $\lambda''_{ijk} = -\lambda''_{ikj}$ . Hence, there are 9 (for each) independent  $\lambda$  and  $\lambda''$  couplings whilst 27 independent  $\lambda'$  couplings remain. Altogether 45 extra free parameters are grafted to minimal SUSY models.

In order to comply with the remarkable stability of the proton and the absence of  $n - \bar{n}$  oscillations, it is sufficient to impose the baryon number conservation ( $B$ -parity) as a viable<sup>5</sup> and less restrictive discrete symmetry. This implies  $\lambda'' = 0$  in Eq. 1. This might be seen as a “natural” choice for cosmology where the observed matter/antimatter asymmetry imposes much more severe constraints<sup>6</sup> on  $\lambda''$  than on  $\lambda$  or  $\lambda'$ . On the contrary,  $I'$  terms do not unavoidably suffer from cosmological constraints<sup>6</sup> and are even required for baryon asymmetry genesis in some cosmological models with first order electroweak phase transition<sup>7</sup>. Provided that baryon number is effectively conserved at low energy, sizeable  $\lambda'$  couplings are consistent with GUT's, Supergravity and Superstring theories<sup>3,5,8</sup>.

### 3 Phenomenology at HERA

#### 3.1 Lagrangian and Free Parameters

Of particular interest for HERA are the terms  $\lambda'_{ijk} L_i Q_j \bar{D}_k$  in the  $\mathcal{H}_p$  extension of the MSSM which allow for  $I'$  processes. This was first realized and was investigated theoretically in Ref.<sup>9</sup> which motivated early experimental searches<sup>10</sup>. These terms correspond in expanded field notation to the Lagrangian:

$$\begin{aligned} \mathcal{L}_{L_i Q_j \bar{D}_k} = \lambda'_{ijk} & \left[ -\tilde{e}_L^i u_L^j \bar{d}_R^k - e_L^i \tilde{u}_L^j \bar{d}_R^k - (\tilde{e}_L^i)^c u_L^j \bar{d}_R^{k*} \right. \\ & \left. + \tilde{\nu}_L^i d_L^j \bar{d}_R^k + \nu_L \tilde{d}_L^j \bar{d}_R^k + (\tilde{\nu}_L^i)^c d_L^j \bar{d}_R^{k*} \right] + \text{h.c.} \quad (2) \end{aligned}$$

<sup>b</sup>A bilinear term  $\mu L_i H_2$  involving the Higgs doublet  $H_2$  is also allowed<sup>3</sup> but not considered further here.

where the superscripts  $c$  denote the charge conjugate spinors and the  $*$  the complex conjugate of scalar fields. The ‘R’ and ‘L’ indices for the scalars distinguish independent fields describing superpartners of right- and left-handed fermions respectively. Among the 27 possible  $\lambda'_{ij,k}$  couplings, the cases  $i = 1$  can lead to direct squark resonant production through  $e$ - $q$  fusion and are thus of special interest at HERA. In the following we assume conservatively that one of the  $\lambda'$  dominates. Recent investigations<sup>11,14,12,13</sup> have shown that a new and rich phenomenology (different for  $e^-$  and  $e^+$  beams) emerges when considering the full complexity of the mixing in the gaugino-higgsino sector of the theory.

The masses of the new squark and slepton scalars are treated here as free parameters. In the gaugino-higgsino sector, there are four neutralino  $\chi_{1,2,3,4}^0$  and two chargino  $\chi_{1,2}^\pm$  mass eigenstates. The  $\chi_m^0$  are mixed states of the photino  $\tilde{\gamma}$ , the zino  $\tilde{Z}$  and the SUSY partners  $\tilde{H}_1^0$  and  $\tilde{H}_2^0$  of the two neutral Higgs fields. The  $\chi_n^\pm$  are mixed states of the winos  $\tilde{W}^\pm$  and of the SUSY partners of the charged Higgs fields. The masses and couplings of the  $\chi^0$  and  $\chi^\pm$  are calculated in terms of the MSSM basic parameters :

- $M_1$  and  $M_2$ , the  $U(1)$  and  $SU(2)$  soft-breaking gaugino mass terms;
- $\mu$ , the mixing parameter associated to Higgs superfields;
- $\tan\beta \equiv v_2/v_1$ , the ratio of the vacuum expectation values of the two neutral Higgs fields.

The number of free parameters is reduced by assuming a relation at the Grand Unification (GUT) scale between  $M_1$  and  $M_2$ , namely  $M_1 = 5/3 M_2 \tan^2 \theta_W$  where  $\theta_W$  is the weak mixing angle. No other GUT relations are used and in particular the gluino ( $\tilde{g}$ ) mass is left free. In the following, we moreover assume to simplify that :

- all squarks (except the stop) are quasi-degenerate in mass;
- gluinos are heavier than the squarks such that real  $\tilde{q} \rightarrow q + \tilde{g}$  decays are kinematically forbidden;
- the LSP is the lightest neutralino  $\chi_1^0$ .

The latter is assumed notwithstanding the fact that there are no compelling cosmological constraint in  $\tilde{R}_p$  models which imposes that the (generally) unstable LSP be neutral and colourless. It is nevertheless justified since other possible choices for the LSP (e.g.  $\tilde{g}$  or  $\chi^\pm$ ) would not significantly change the search and analysis strategy. Other possible LSP choices will therefore only be briefly discussed.

Table 1: Squark production processes at HERA ( $e^+$  beam) via a R-parity violating  $\lambda'_{1jk}$  coupling.

$\lambda'_{1jk}$	Production processes	
111	$e^+ + \bar{u} \rightarrow \tilde{d}_R$	$e^+ + d \rightarrow \tilde{u}_L$
112	$e^+ + \bar{u} \rightarrow \tilde{s}_R$	$e^+ + s \rightarrow \tilde{u}_L$
113	$e^+ + \bar{u} \rightarrow \tilde{b}_R$	$e^+ + b \rightarrow \tilde{u}_L$
121	$e^+ + \bar{c} \rightarrow \tilde{d}_R$	$e^+ + d \rightarrow \tilde{c}_L$
122	$e^+ + \bar{c} \rightarrow \tilde{s}_R$	$e^+ + s \rightarrow \tilde{c}_L$
123	$e^+ + \bar{c} \rightarrow \tilde{b}_R$	$e^+ + b \rightarrow \tilde{c}_L$
131	$e^+ + \bar{t} \rightarrow \tilde{d}_R$	$e^+ + d \rightarrow \tilde{t}_L$
132	$e^+ + \bar{t} \rightarrow \tilde{s}_R$	$e^+ + s \rightarrow \tilde{t}_L$
133	$e^+ + \bar{t} \rightarrow \tilde{b}_R$	$e^+ + b \rightarrow \tilde{t}_L$

### 3.2 Squark Resonant Production

Single squark production through resonant  $e$ - $q$  fusion is illustrated in Fig. 1 for  $\lambda'_{111} \neq 0$ . By gauge symmetry, only  $\tilde{u}_L$ -like or  $\tilde{d}_R$ -like squarks (or their charge conjugates) can be produced in  $ep$  collisions. The production of “left” squarks is the dominating process if HERA delivers positrons, since the fusion occurs via a  $d$  valence quark. On the contrary, with electrons in the initial state, mainly “right” squarks are produced. This dichotomy has important consequences since “left” and “right” squarks have different allowed or dominant decay modes as will be seen in the following sections. In particular, new exotic final state topologies might have sizeable contributions in  $e^+p$  collisions.

In contrast to most indirect processes, HERA offers a high sensitivity to any of the nine  $\lambda'_{1jk}$  couplings. The production processes allowed for each  $\lambda'_{1jk}$  are listed in Table 1 for an  $e^+$  beam. With an  $e^-$  beam, the corresponding charge conjugate processes are  $e^- u_j \rightarrow \tilde{d}_R^k$  ( $e^- \bar{d}_k \rightarrow \tilde{u}_L^j$ ) for  $u$ -like ( $d$ -like)

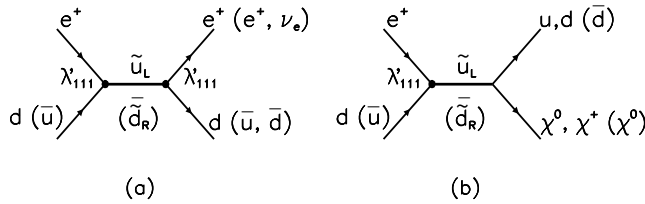
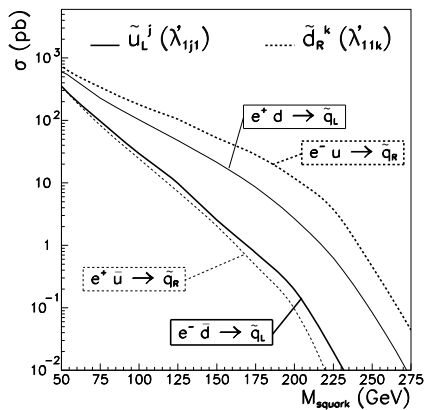


Figure 1:  $H_p$  resonant production of  $\tilde{u}_L$  or  $\tilde{d}_R$  squarks in  $e^+p$  collisions with subsequent (a)  $H_p$  decay or (b) gauge decay involving a (generally) unstable gaugino-higgsino ( $\chi^0$  or  $\chi^+$ ).

Figure 2: Squark production cross-sections in  $ep$  collisions for a coupling  $\lambda' = 0.1$ .



quarks of the  $j$ th ( $k$ th) generation. Squark production via  $\lambda'_{1j1}$  is especially interesting in  $e^+p$  collisions as it involves a valence  $d$  quark, whilst  $\lambda'_{11k}$  are best probed with an  $e^-$  beam since squark production then involves a valence  $u$  quark. This is seen in Fig. 2 which shows the production cross-sections  $\sigma_{\tilde{q}}$  for “up”-like squarks  $\tilde{u}_L^j$  via  $\lambda'_{1j1}$ , and for “down”-like squarks  $\tilde{d}_R^k$  via  $\lambda'_{11k}$ , each plotted for coupling values of  $\lambda' = 0.1$ . In the narrow width approximation, these are simply expressed as

$$\sigma_{\tilde{q}} = \frac{\pi}{4s} \lambda'^2 q' \left( \frac{M^2}{s} \right) \quad (3)$$

where  $\sqrt{s} = \sqrt{4E_e^0 E_p^0} \simeq 300$  GeV is the energy available in the CM frame for incident beam energies of  $E_e^0 = 27.5$  GeV and  $E_p^0 = 820$  GeV, and  $q'(x)$  is the probability to find the relevant quark (e.g. the  $d$  for  $\tilde{u}_L$  and the  $\bar{u}$  for  $\tilde{d}_R$ ) with momentum fraction  $x = M^2/s \simeq M_{\tilde{q}}^2/s$  in the proton. Hence the production cross-section approximately scales in  $\lambda'^2$ . The full kinematic domain will be probed at HERA for squarks<sup>c</sup> with couplings weaker than the electromagnetic coupling (i.e.  $\lambda' < \sqrt{4\pi\alpha_{em}}$ ) given an integrated luminosity of  $\mathcal{L}_{HERA} \simeq 500\text{pb}^{-1}$ .

<sup>c</sup>Squarks can also be created by pair at HERA via  $\gamma$ -gluon fusion or in associated  $\tilde{e}\tilde{q}$  production via  $t$ -channel exchange of a  $\chi_m^0$ . The former process was studied by the H1 Collaboration<sup>12</sup> for the  $\tilde{t}$  and  $9 \lesssim M_{\tilde{q}} \lesssim 24.4$  GeV could be excluded for  $\lambda'_{13k} \times \cos\theta_t > 10^{-4}$  where  $\theta_t$  is a mass mixing angle. The latter was studied in Ref.<sup>15</sup> where it was shown that  $\lambda' \ll \sqrt{4\pi\alpha_{em}}$  could be probed for couplings to any lepton generations for masses up to  $M_{\tilde{e}} + M_{\tilde{q}} \simeq 200$  GeV.

### 3.3 Squark Decays

The squarks decay either via their Yukawa coupling into ordinary matter fermions, or in a first step via their gauge coupling into a quark and a neutralino  $\chi_m^0$  or a chargino  $\chi_n^+$ . The former modes are henceforward called “squark  $\tilde{R}_p$  decays” and the latter “squark gauge decays”.

**$\tilde{R}_p$  decays of squarks:** In cases where both production and decay occurs through a  $\lambda'_{1jk}$  coupling (e.g. Fig. 1a for  $\lambda'_{111} \neq 0$ ), the squarks behave as scalar leptoquarks<sup>16,17</sup>. For  $\lambda'_{111} \neq 0$ , the  $\tilde{d}_R$  resembles on event-by-event (but not in total intrinsic width) the  $\tilde{S}^0$  leptoquark and decays in either  $e^+ + \bar{u}$  or  $\nu_e + \bar{d}$  while the  $\tilde{u}_L$  resembles the  $\tilde{S}_{1/2}$  and only decays into  $e^+ \bar{d}$ . Of course this resemblance with leptoquarks possessing pure chiral couplings is only superficial since the  $\tilde{q}_L$  and  $\tilde{q}_R$  in the MSSM always mix at some level and will be subject to specific indirect constraints as discussed further in 5. The partial decay width reads :

$$\Gamma_{\tilde{q} \rightarrow \tilde{R}_p} = \Gamma_{\tilde{u}_L \rightarrow e^+ \bar{d}} = \Gamma_{\tilde{d}_R \rightarrow e^+ \bar{u}} = \Gamma_{\tilde{d}_R \rightarrow \nu \bar{d}} = \frac{1}{16\pi} \lambda'_{111}{}^2 M_{\tilde{q}} \quad (4)$$

so that squark  $\tilde{R}_p$  decays will mainly contribute at high mass for large Yukawa coupling values  $\lambda'$ . Hence, the final state signatures consist of a lepton and a jet and are, event-by-event, indistinguishable from the SM neutral (NC) and charged current (CC) deep inelastic scattering (DIS).

**Gauge decays of squarks:** The MSSM Lagrangian contains terms coupling a sfermion to an ordinary fermion and a gaugino-higgsino. The partial widths for squark gauge decays depend on MSSM parameters via the composition of the neutralinos or charginos.

Both  $\tilde{q}_L$  and  $\tilde{q}_R$  squarks can decay via  $\tilde{q} \rightarrow q\chi_m^0$ . The partial width of the  $\tilde{q} \rightarrow q\chi_m^0$  decay is calculated to be

$$\Gamma_{\tilde{q} \rightarrow q\chi_m^0} = \frac{1}{8\pi} (A^2 + B^2) M_{\tilde{q}} \left( 1 - \frac{M_{\chi_m^0}^2}{M_{\tilde{q}}^2} \right)^2 \quad (5)$$

where for the  $\tilde{u}_L$  :

$$A = \frac{gM_u N_{m4}}{2M_W \sin \beta} \quad , \quad B = ee_u N'_{m1} + g(0.5 - e_u \sin^2 \theta_W) \frac{N'_{m2}}{\cos \theta_W}, \quad (6)$$

and for the  $\tilde{d}_R$  :

$$A = \frac{gM_d}{2M_W \cos \beta} N_{m3} \quad , \quad B = ee_d N'_{m1} - \frac{ge_d \sin^2 \theta_W}{\cos \theta_W} N'_{m2} \quad (7)$$

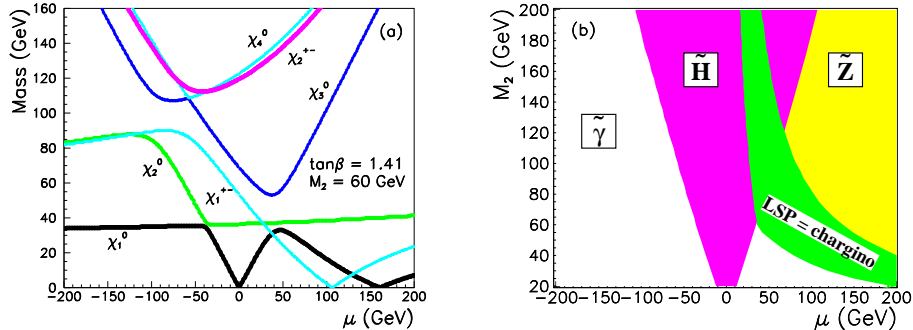


Figure 3: (a) Physical masses of the  $\chi_i^0$  and  $\chi_i^{\pm}$  as a function of  $\mu$  for  $\tan\beta = \sqrt{2}$  and  $M_2 = 60$  GeV; (b) Main component of the LSP for  $\tan\beta = 1$

and where  $N_{mn}$  ( $N'_{mn}$ ) is the transport matrix which diagonalizes the neutralino mass matrix in the  $\tilde{A} - \tilde{W}_3$  ( $\tilde{\gamma} - \tilde{Z}$ ) basis. In practice, the  $\chi_m^0$  masses and the exact values of the “chiral” couplings  $A$  and  $B$  depend on the basic MSSM parameters  $M_2$ ,  $\mu$  and  $\tan\beta$ , or equivalently on the  $\chi_1^0$  nature in terms of relative  $\tilde{\gamma}$ ,  $\tilde{Z}$  and  $\tilde{H}$  components<sup>18,20</sup>.

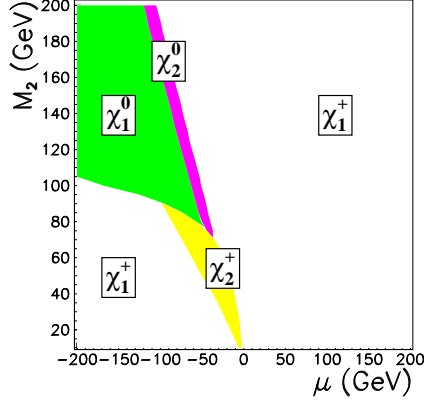
The dependence of the  $\chi_m^0$  mass on the  $\mu$  parameter is shown in Fig. 3a for fixed  $M_2$  and  $\tan\beta$ . The dominant component ( $\tilde{\gamma}$ ,  $\tilde{Z}$  or  $\tilde{H}$ ) of the lightest state  $\chi_1^0$  is shown in Fig. 3b. For a  $\tilde{\gamma}$ -like LSP, i.e. a  $\chi_1^0$  dominated by its photino component, the  $\tilde{q}$  to  $q + \tilde{\gamma}$  coupling is proportional to the  $q$  electric charge (i.e.  $A = 0$  and  $B = ee_q$  for a pure  $\tilde{\gamma}$ ) and the  $\tilde{q}$  partial width reduces to

$$\Gamma_{\tilde{q} \rightarrow q + \tilde{\gamma}} = \frac{1}{8\pi} e^2 e_q^2 M_{\tilde{q}} \left( 1 - \frac{M_{\tilde{\gamma}}^2}{M_{\tilde{q}}^2} \right)^2. \quad (8)$$

In such a case, more than 90% of the  $\tilde{q} \rightarrow q\chi_m^0$  decays will involve the  $\chi_1^0$ . A similar partial branching ratio holds for a  $\tilde{H}$ -like LSP with a relatively large  $\tilde{Z}$  component (e.g. in the  $\tilde{H}$  region close to the  $\tilde{Z}$  region in Fig. 3b). For a  $\tilde{Z}$ -like LSP ( $A = 0$  and  $B \propto g$  for a pure  $\tilde{Z}$ ) this branching ratio reduces to  $20\% < \mathcal{B} < 80\%$ . Decays involving the LSP are negligible only in the  $\tilde{H}$  domain ( $A \propto M_q$  and  $B = 0$  for a pure  $\tilde{H}$ ) extending to negative  $\mu$ 's adjacent to the  $\tilde{\gamma}$  domain (Fig. 3b).

(Almost) only the  $\tilde{q}_L$  are allowed by gauge symmetry to decay into  $q'\chi_n^+$ . This is because the  $SU(2)_L$  symmetry which implies in the SM that the right handed fermions do not couple to the  $W$  boson also forbids a coupling of  $\tilde{q}_R$

Figure 4: Dominant gauge decay of a 150 GeV  $\tilde{u}_L$  squark, for  $\tan\beta = 1$ .



to the  $\tilde{W}$ . The  $\tilde{q}_R$  decays involving the chargino is only possible through the  $\tilde{H}^+$  component of the  $\chi^+$  in which case the coupling is proportional to the  $q'$  mass. Hence the decay  $\tilde{q}_R \rightarrow q' \chi_n^+$  is strongly suppressed for a  $\tilde{q}_R$  of the first or second generation. The partial width of the  $\tilde{u}_L \rightarrow d \chi_n^+$  decay is obtained from (5) with the interchange  $M_{\chi_n^0} \rightarrow M_{\chi_n^+}$  and with :

$$A = \frac{gV_{n1}}{\sqrt{2}} \quad B = \frac{-gM_d U_{n2}}{2M_W \cos\beta} , \quad (9)$$

$V$  and  $U$  being matrices defining the composition of the charginos<sup>18</sup>. The regions of the  $M_2$  vs  $\mu$  plane where the  $\tilde{u}$  decays involving a chargino dominate are shown in Fig. 4. In most of the parameter space, the  $\tilde{u}_L$  squarks will mainly undergo a decay involving a chargino if kinematically allowed. The mass dependence of the  $\chi_n^+$  states on the  $\mu$  parameter is shown in Fig. 3a for fixed  $M_2$  and  $\tan\beta$ .

#### 3.4 Gaugino-Higgsino Decays

In  $\tilde{R}_p$  SUSY models with  $\lambda'_{jk} \neq 0$ , the LSP will undergo one of the following decays :  $\chi_1^0 \rightarrow \nu \bar{d}_k d_j$ ,  $\chi_1^0 \rightarrow e^+ \bar{u}_j d_k$  or  $\chi_1^0 \rightarrow e^- u_j \bar{d}_k$ . Representative diagrams are given in Fig. 5. The relevant matrix elements for such decays can be found in Ref.<sup>15</sup>. They depend on the coupling  $\lambda'$ , but also on the parameters  $M_2$ ,  $\mu$  and  $\tan\beta$ . This dependence is shown in Fig. 6a for the LSP decay  $\chi_1^0 \rightarrow e^\pm q \bar{q}'$ . Such decay modes are seen to be dominant ( $63\% < \mathcal{B}_R < 88\%$ ) if the  $\chi_1^0$  is  $\tilde{\gamma}$ -like in which case both the “right” and the “wrong” sign lepton (compared to the incident beam) are equally probable. This leads to largely background

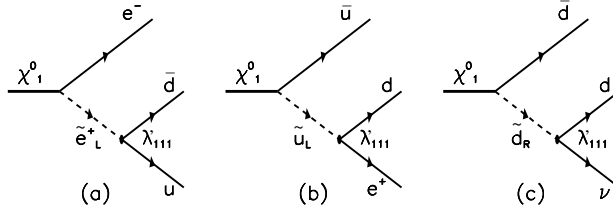


Figure 5: Example diagrams of the LSP decays  $\chi_1^0 \rightarrow lqq'$  involving a  $\tilde{H}_p$  Yukawa coupling.

free striking signatures for  $\cancel{L}$ . The decay  $\chi_1^0 \rightarrow \nu \bar{d}_k d_j$  will dominate if the  $\chi_1^0$  is  $\tilde{Z}$ -like. A  $\tilde{H}$ -like  $\chi_1^0$  will most probably be long lived and escape detection since its coupling to fermion-sfermion pairs is proportional to the fermion mass<sup>18</sup>. This is illustrated in Fig. 6b, which shows the flight distance  $c\tau_0$  of the  $\chi_1^0$  in the plane  $(M_2, \mu)$  for  $\lambda' = 0.1$ . The  $c\tau_0$  exceeds 1 m in most of the  $\tilde{H}$ -like domain surrounding the singularity at  $\mu = 0$  where  $M_{\chi_1^0} = 0$  at tree level. Hence processes involving a higgsino-like  $\chi_1^0$  will be affected by an imbalance in transverse momenta.

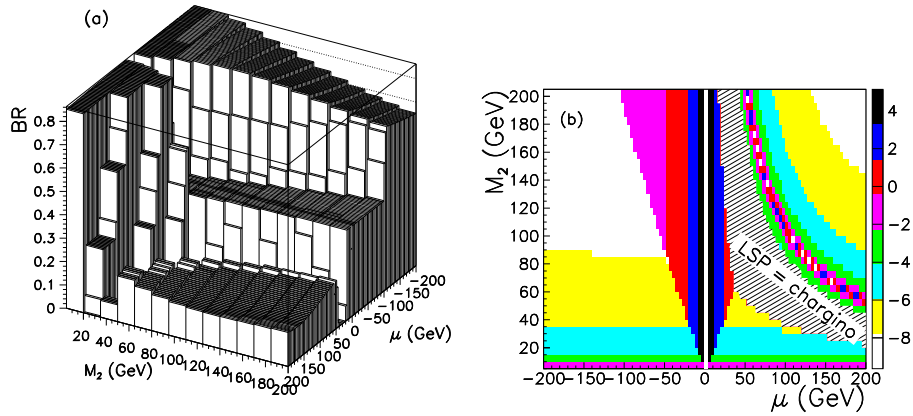


Figure 6: (a) LSP ( $\chi_1^0$ ) decay branching ratio into charged leptons (i.e.  $e^\pm + jets$ ), as a function of  $\mu$  and  $M_2$  for sfermion masses  $M_{\tilde{f}} = 150$  GeV and  $\tan\beta = 1$ ; (b)  $\log c\tau_0$  (m) of the LSP with  $\lambda' = 0.1$ , the LSP mass is vanishingly small around  $\mu = 0$  and along the ridge at large  $\mu + M_2$ .

### 3.5 Chargino Decays

R-parity conserved  $\chi^+$  decays into a  $\chi^0$  and two matter fermions, have been investigated in detail in<sup>19</sup>, where the relevant matrix elements can be found.

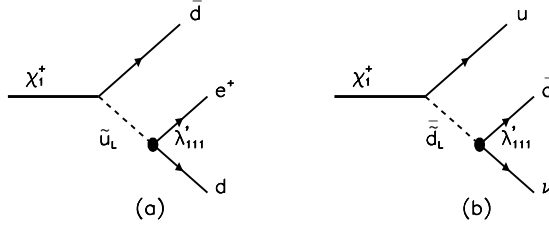


Figure 7: Example diagrams for the  $\chi_1^+$  decays  $\chi_1^+ \rightarrow lqq'$  involving a  $\tilde{H}_p$  Yukawa coupling.

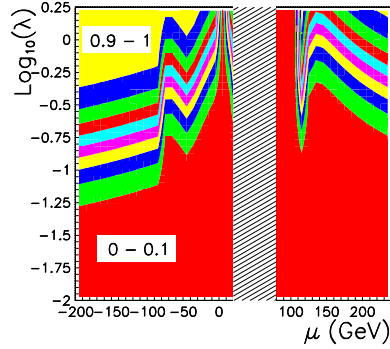
New decay modes of the  $\chi^+$  into  $e^+ + d_j + \bar{d}_k$  or  $\nu_e + u_j + \bar{d}_k$  are allowed by the  $\tilde{H}_p$  couplings  $\lambda'_{1jk}$  as illustrated in Fig. 7. The calculation of the branching ratio of the  $\chi_1^+$  into these  $\tilde{H}_p$  modes using the partial widths calculated from the relevant matrix elements was performed in<sup>20</sup>. The partial width obtained after numerical integration over phase space is shown in Fig. 8.

The  $\tilde{H}_p$  decays of the  $\chi_1^+$  will mainly dominate over MSSM decays as soon as  $\lambda'$  is not too small. For  $\chi_1^0 \simeq \tilde{\gamma}$ ,  $\tilde{H}_p$  decays of the chargino dominate over MSSM modes for coupling values above  $\simeq 0.25$ , which is typically HERA's sensitivity limit with current luminosity.

### 3.6 Observable Final States

Taking into account the dependence on the nature of the  $\chi_1^0$ , the possible decay chains of the  $\tilde{u}_L$  and  $\tilde{d}_R$  squarks can be classified into eight distinguishable event topologies listed in Tables 2 and 3 and labelled S1 to S8. The S1 and S2 classes cover  $\tilde{H}_p$  squark decays. The S3 and S4 classes are squark gauge decay topologies not accompanied by escaping transverse momenta  $\cancel{p}_\perp$ , while

Figure 8:  $\tilde{H}_p$  chargino decay branching ratio as a function of  $\lambda'_{111}$  and  $\mu$ , for  $M_2 = 80$  GeV,  $\tan\beta = 1$  and sfermions masses = 150 GeV; the hatched domain corresponds to  $\mu$  values for which  $M(\chi_1^+) < M(\chi_1^0)$ .



Class	$\chi_1^0$ nature	Decay processes	Signature
S1	$\tilde{\gamma}, \tilde{Z}, \tilde{H}$	$\tilde{q} \xrightarrow{\lambda'} e^+ q'$	$e^+ + 1 \text{ jet}$
S2	$\tilde{\gamma}, \tilde{Z}, \tilde{H}$ $\tilde{H}$	$\tilde{d}_R \xrightarrow{\lambda'} \nu_e \bar{d}$ $\tilde{q} \longrightarrow q \chi_1^0$	$\cancel{P}_\perp + 1 \text{ jet}$
S3	$\tilde{\gamma}, \tilde{Z}$ $\tilde{\gamma}, \tilde{Z}, \tilde{H}$ $\tilde{\gamma}, \tilde{Z}$	$\tilde{q} \longrightarrow q \chi_1^0$ $\xrightarrow{\lambda'} e^+ \bar{q}' q''$ $\tilde{u}_L \longrightarrow d \chi_1^+$ $\xrightarrow{\lambda'} e^+ d \bar{d}$ $\tilde{u}_L \longrightarrow d \chi_1^+$ $\xrightarrow{\lambda'} W^+ \chi_1^0$ $\xrightarrow{\lambda'} e^+ \bar{q}' q''$ $\xrightarrow{\lambda'} q \bar{q}'$	$e^+ + \text{jets}$
S4	$\tilde{\gamma}, \tilde{Z}$ $\tilde{\gamma}, \tilde{Z}$	$\tilde{q} \longrightarrow q \chi_1^0$ $\xrightarrow{\lambda'} e^- \bar{q}' q''$ $\tilde{u}_L \longrightarrow d \chi_1^+$ $\xrightarrow{\lambda'} W^+ \chi_1^0$ $\xrightarrow{\lambda'} e^- \bar{q}' q''$ $\xrightarrow{\lambda'} q \bar{q}'$	$e^- + \text{jets}$

Table 2: Squark decays in  $\tilde{H}_p$  SUSY classified per distinguishable event topologies (Part I). The dominant component of the  $\chi_1^0$  for which a given decay chain is relevant is given in the second column. The list of processes contributing to a given event topology is here representative but not exhaustive.

those with large  $\cancel{P}_\perp$  are covered by classes S5 to S8. It is interesting to note that the final state classification discussed here should not be dramatically affected when relaxing the hypothesis of section 3.1, e.g. in models where the  $\tilde{g}$  are lighter than the  $\tilde{q}$ , or where the LSP is the  $\chi_1^+$ .

Assuming  $M_{\tilde{g}} < M_{\tilde{q}}$ , the decay  $\tilde{q} \rightarrow q + \tilde{g}$  will generally dominate. If the  $\tilde{g}$  is the LSP, the  $\tilde{q}$  decay will be followed by the  $\tilde{H}_p$  decay  $\tilde{g} \rightarrow q + q' + e^\pm$  or  $\tilde{g} \rightarrow q + \bar{q} + \nu$ . In such a case, possible final states contain several jets and either one electron or  $\cancel{P}_\perp$ . These topologies correspond to channels S3 and S5, previously considered. If  $M_{\tilde{q}} > M_{\tilde{g}}$ , with the LSP being the lightest neutralino, the  $\tilde{g}$  arising from squark decay will undergo  $\tilde{g} \rightarrow q + \tilde{q}$ , the latter squark being off-shell. Possible final states are similar to those listed above, but more jets would be expected. Assuming now that the LSP is the  $\chi_1^+$  (see the relevant MSSM parameters in Fig. 3b), a new event topology would only emerge for

Class	$\chi_1^0$ nature	Decay processes	Signature
S5	$\tilde{\gamma}, \tilde{Z}$	$\tilde{q} \longrightarrow q \chi_1^0$ $\xrightarrow{\lambda'} \nu \bar{q}' q'$	$\cancel{p}_\perp + \text{jets}$
	$\tilde{\gamma}, \tilde{Z}$	$\tilde{u}_L \longrightarrow d \chi_1^+$ $\hookrightarrow W^+ \chi_1^0$ $\xrightarrow{\lambda'} \nu \bar{q}' q'$ $\hookrightarrow q \bar{q}'$	
	$\tilde{\gamma}, \tilde{Z}, \tilde{H}$	$\tilde{u}_L \longrightarrow d \chi_1^+$ $\xrightarrow{\lambda'} \nu u \bar{d}$	
	$\tilde{H}$	$\tilde{u}_L \longrightarrow d \chi_1^+$ $\hookrightarrow W^+ \chi_1^0$ $\hookrightarrow q \bar{q}'$	
S6	$\tilde{H}$	$\tilde{u}_L \longrightarrow d \chi_1^+$ $\hookrightarrow W^+ \chi_1^0$ $\hookrightarrow l^+ \nu$	$e^+$ or $\mu^+$ , $\cancel{p}_\perp + 1 \text{ jet}$
S7	$\tilde{\gamma}, \tilde{Z}$	$\tilde{u}_L \longrightarrow d \chi_1^+$ $\hookrightarrow W^+ \chi_1^0$ $\xrightarrow{\lambda'} e^\pm \bar{q}' q''$ $\hookrightarrow l^+ \nu$	$e^\pm$ + $e^+$ or $\mu^+$ , $\cancel{p}_\perp + \text{jets}$
S8	$\tilde{\gamma}, \tilde{Z}$	$\tilde{u}_L \longrightarrow d \chi_1^+$ $\hookrightarrow W^+ \chi_1^0$ $\xrightarrow{\lambda'} \nu \bar{q}' q'$ $\hookrightarrow l^+ \nu$	$e^+$ or $\mu^+$ , $\cancel{p}_\perp + \text{jets}$

Table 3: Squark decays in  $R_p$  SUSY classified per distinguishable event topologies (Part II).

a relatively stable  $\chi_1^+$  which could behave as a ‘‘heavy muon’’. However, the time of flight of the  $\chi_1^+$ , obtained<sup>20</sup> from the integration over phase space, reads as :

$$\tau = \frac{4\pi}{g^2} \frac{1}{|V_{11}|^2} \frac{1}{\lambda'^2} (8 \times 64\pi^2) \left( \frac{M_{\tilde{q}}}{M_{\chi_1^+}} \right)^4 \frac{1}{M_{\chi_1^+}} \quad (10)$$

which numerically leads to :

$$\tau = (2.5 \cdot 10^{-15} \text{ s}) \left( \frac{5 \cdot 10^{-3}}{\lambda'} \right)^2 \frac{1}{|V_{11}|^2} \left( \frac{100 \text{ GeV}}{M_{\chi_1^+}} \right)^5 \left( \frac{M_{\tilde{f}}}{150 \text{ GeV}} \right)^4. \quad (11)$$

From this formula one obtains that the relevant parameter space for the  $\chi_1^+$  to decay outside the detector ( $\gtrsim 1\text{m}$ ), is already excluded from the intrinsic  $Z^0$  width measurement at CERN <sup>21</sup>.

#### 4 Analysis and Exclusion Limits From Direct Searches at HERA

A set of event selection cuts has been developed and discussed in detail in <sup>10,12</sup>. For S1 and S3 (or S4), the DIS NC background is strongly suppressed by requiring a high  $P_\perp e^\pm$  found at high  $y_e$ , where  $y_e$  is the usual Bjorken variable for DIS. It is calculated in the laboratory frame (L-frame) as  $y_e^L = 1 - E_e/E_e^0 \sin^2 \theta_e$  where  $E_e$  ( $E_e^0$ ) is the scattered (incident) electron energy and  $\theta_e$  the scattering angle. For S1, the  $y_e$  distribution is flat since the scalar particle decays uniformly in the  $e - q$  center-of-mass frame (CM-frame) and given that  $y_e^L = y_e^{CM} = 1/2(1 + \cos \theta_e^{CM})$  where  $\theta_e^{CM}$  is the electron polar angle in the CM-frame. For S3, the  $y_e^L$  distribution appears strongly shifted towards largest values since the final state  $e$  carries only a fraction of the momentum of the  $\chi$  which emerged from the  $\tilde{q}$  two-body decay. In each case the  $y_e$  distributions are in contrast to the  $1/y_e^2$  spectrum expected for the DIS NC background at fixed quark momentum fraction  $x$ .

For S3 the early H1 analysis <sup>12</sup> has been recently improved <sup>22</sup> in two ways. First, the expected peak resolution for the reconstructed squark mass is improved by a factor  $\simeq 2$  by imposing overall kinematic constraints. Second, the different (spin dependent) characteristics of the angular distributions for the expected signal and the DIS NC background is better exploited. A  $y_{jet}^{CM}$  is calculated from the highest  $P_\perp$  jet found in the azimuthal hemisphere opposite to the  $e$  as  $y_{jet}^{CM} = 1/2(1 + \cos \theta_{jet}^{CM})$  where  $\theta_{jet}^{CM}$  is the jet polar angle in the CM-frame. For DIS NC processes at lowest order in QCD, one expects then

Figure 9: Distribution of the variable  $\Sigma y$  for neutral current DIS processes, and for a simulation of 75 GeV squarks undergoing gauge decays involving 20 GeV neutralinos; the vertical line is the cut used in the H1 analysis <sup>22</sup>.

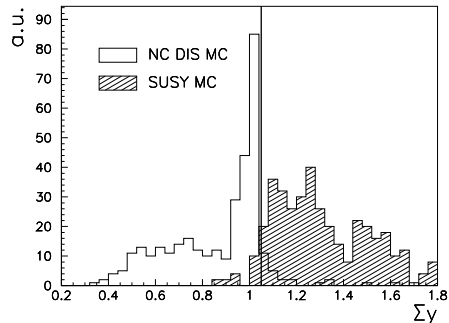
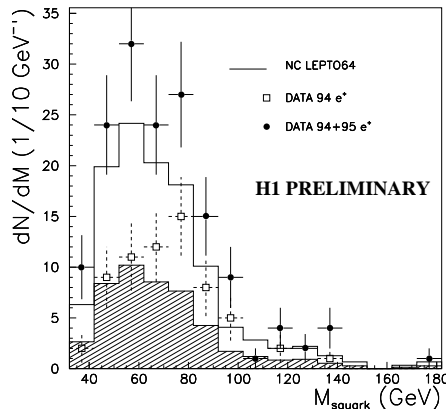


Figure 10: Mass spectra for squarks in the S3 channel for 1994 and 1994+1995 H1 data.



$\sum y = y_e^L + y_{jet}^{CM} = y_e^{CM} + y_{jet}^{CM} \simeq 1$  and QCD radiation will produce tails mostly towards  $\sum y \lesssim 1$ . This is shown Fig. 9 where it is seen that a cut  $\sum y > 1.05$  removes most of this DIS NC background while retaining S3 signal events.

Good signal detection efficiencies are obtained in S1 and S3 classes, reaching  $\sim 70\%$  for S1 and up to  $\sim 60\%$  depending on  $M_{\chi_1^0}$  for S3. The S4 topology with a wrong sign lepton in the final state is quasi-background free. Event candidates in classes S2 and S5 to S8 have a large  $p_\perp$ . Classes S2 and S5 suffer from DIS CC background and from tails of photoproduction background. The S6 to S8 topologies have one or many leptons in the final states and are thus quasi-background free. Typical signal detection efficiencies<sup>12</sup> reach  $\sim 30\% \rightarrow 80\%$  in these channels. An excellent agreement is found between observations and background expectations in all channels. In particular no event candidate was found in the S4 class. A slight ( $\sim 2.4\sigma$ ) excess around  $M_{\tilde{q}} = 70$  GeV which was observed<sup>12,22</sup> in the H1 1994 data in the S3 class (like-sign  $e$ ) of events is seen in Fig. 10 to be essentially washed away by the addition of the new 1995 data. An intriguing  $e^+p \rightarrow \mu^+ + jet(s) + X$  found in the 1994 data sample<sup>23</sup> belongs to S6 (or eventually S8) event topologies<sup>23</sup>. No such event candidate was found with the 1995 data.

Combining all channels, exclusion limits have been derived by the H1 experiment using the 1994 data sample. The relative contributions of the squark  $\tilde{R}_p$  and gauge decays are shown in Fig. 11. Gauge decays are seen to dominate through most of the accessible mass range. Only large Yukawa couplings can be probed at largest masses and thence  $\tilde{R}_p$  decays dominate. The shape of the

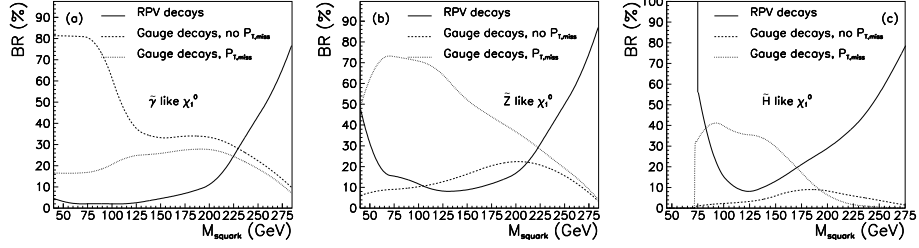


Figure 11: Squark decay branching ratio as a function of squark mass, integrated over three distinct set of event topologies for  $\tan\beta = 1$  and  $M_{\chi_1^0} = 40$  GeV for a  $\chi_1^0$  with dominant (a)  $\tilde{\gamma}$ , (b)  $\tilde{Z}$  and (c)  $\tilde{H}$  components. The branching ratios are calculated for values of the  $\lambda'$  at the boundary of the excluded domains obtained by the H1 experiment (see Fig. 12).

curves in Fig. 11 is only distorted at lowish mass (e.g.  $M_{\tilde{q}} \lesssim 75$  GeV) when convoluting with signal detection efficiencies.

The results for  $\lambda'_{1j1}$  combining all contributing channels are shown in Fig. 12 for  $M_{\chi_1^0} = 40$  GeV. The existence of squarks with  $\tilde{B}_p$  Yukawa couplings  $\lambda'_{1j1}$  is excluded for masses up to  $\sim 220$  GeV (240 GeV for  $M_{\chi_1^0} \simeq 160$  GeV) for coupling values  $\lambda'_{1j1} \gtrsim \sqrt{4\pi\alpha_{em}}$ . The Fig. 13 shows the excluded domains

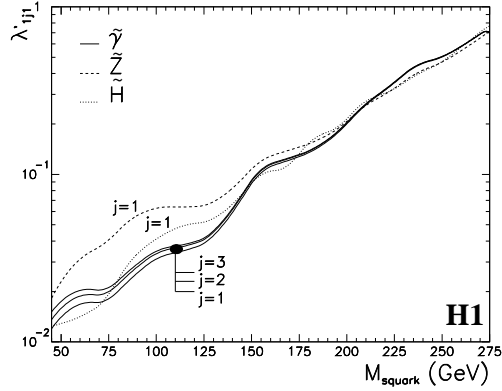
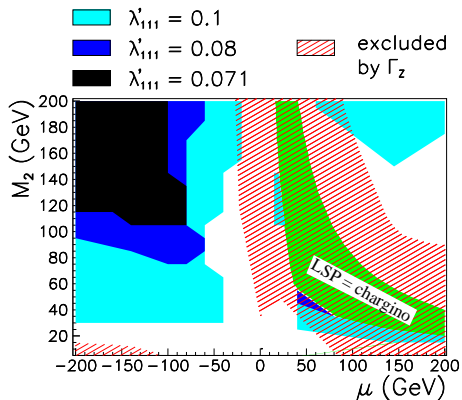


Figure 12: Exclusion upper limits at 95% CL on  $\lambda'_{1j1}$  (regions above the curves excluded).

in the  $M_2$  versus  $\mu$  plane for  $M_{\tilde{q}} = 150$  GeV and  $\lambda'$  values near (or below) the sensitivity limit which is obtained at fixed  $M_{\chi_1^0} = 40$  GeV. To our knowledge,

Figure 13: Excluded domains in the  $M_2$  versus  $\mu$  plane for a  $\lambda'$  close to the upper limits at  $M_{\tilde{q}} = 150$  GeV for  $\tan\beta = 1$ .



no direct searches in the  $\tilde{H}_p$  SUSY framework with  $\lambda' \neq 0$  have been performed yet by  $e^+e^-$  and  $p\bar{p}$  experiments.

From the analysis of the  $\lambda'_{111}$  case involving the  $\tilde{d}_R$  and  $\tilde{u}_L$  squarks, H1 has deduced limits<sup>12</sup>, on the  $\lambda'_{ijk}$  couplings by folding in the proper parton densities. Such limits are given in Table 4 at  $M_{\tilde{q}} = 150$  GeV.

In the presence of two simultaneously non-vanishing Yukawa couplings (e.g.  $\lambda'_{ijk}$  and  $\lambda'_{ikj}$  with  $i \neq 1$ ), resonant  $\tilde{q}$  production at HERA can be directly followed by a  $\tilde{q}$  decay leading to  $\mu + \text{jet}$  or  $\tau + \text{jet}$  signatures. Relevant analyses for these quasi-background free channels have been performed by the H1<sup>16</sup> and ZEUS<sup>27</sup> collaborations. Exclusion limits in the context of  $\tilde{H}_p$  SUSY have been derived by ZEUS<sup>27</sup> based on  $L = 3.8 \text{ pb}^{-1}$  of data and taking into account the branching ratio for gauge decays involving a pure  $\tilde{\gamma}$  LSP (more unfavorable cases of mixed gaugino-higgsino mass eigenstates have not been considered) and assuming that only one type of squark is produced. Under those limiting assumptions, squarks masses up to  $\sim 210$  GeV (depending on the LFV couplings) are excluded by the ZEUS analysis for  $\lambda' \gtrsim \sqrt{4\pi\alpha_{em}}$ .

## 5 Comparison with Indirect Searches

The H1 results are compared in Table 4 to the most severe indirect limits existing.

The most stringent constraints concerns  $\lambda'_{111}$  and is set by the non-observation of neutrinoless double-beta decay ( $\beta\beta 0\nu$ ) which involves only first generation

Table 4: Exclusion upper limits at 95% CL on  $\lambda'_{ijk}$  for  $M_{\tilde{q}} = 150$  GeV and  $M_{\chi_1^0} = 40$  GeV for  $\tilde{\gamma}$ -like and  $\tilde{Z}$ -like  $\chi_1^0$ . Indirect limits have been re-calculated using most recent data and following phenomenology prescriptions of the cited papers. They are scaled to  $M_{\tilde{q}} = 150$  GeV and are quoted at 95% Confidence.

	<u>H1 limits</u>		<u>Indirect limits</u>			[Ref.]
	$\tilde{\gamma}$ -like	$\tilde{Z}$ -like	Value	Process	$\tilde{q}$ -type	
$\lambda'_{111}$	0.056	0.048	0.003	$\beta\beta 0\nu$ decay	$\tilde{u}_L, \tilde{d}_R$	32
			0.011	$K^+$ decays	$\tilde{d}_R$ , CKM mixing	44
$\lambda'_{112}$	0.14	0.12	0.05	CC-universal.		37
			0.063	$e$ - $\mu$ - $\tau$ -universal.	$\tilde{s}_R$	37
			0.011	$K^+$ decays	$\tilde{s}_R$ , CKM mixing	44
$\lambda'_{113}$	0.18	0.15	0.05	CC-universal.		37
			0.063	$e$ - $\mu$ - $\tau$ universal.	$\tilde{b}_R$	37
			0.011	$K^+$ decays	$\tilde{b}_R$ , CKM mixing	44
$\lambda'_{121}$	0.058	0.048	0.56	$D^+$ decays	$\tilde{d}_R$ ,	40
			0.50	$D^0$ decays	$\tilde{d}_R$ ,	40
			0.011	$K^+$ decays	$\tilde{d}_R$ , CKM mixing	44
			0.067	$\nu_e$ -mass	$\tilde{s}$ L-R mixing	42
$\lambda'_{122}$	0.19	0.16	0.011	$K^+$ decays	$\tilde{s}_R$ , CKM mixing	44
			0.56	$D^+$ decays	$\tilde{b}_R$ ,	40
$\lambda'_{123}$	0.30	0.26	0.50	$D^0$ decays	$\tilde{b}_R$ ,	40
			0.011	$K^+$ decays	$\tilde{b}_R$ , CKM mixing	44
			0.32	Atomic $\mathcal{P}$		37
$\lambda'_{131}$	0.06	0.05	0.7	$\Gamma_h/\Gamma_e$ $ ^Z$		43
			0.7	$\Gamma_h/\Gamma_e$ $ ^Z$		43
$\lambda'_{132}$	0.22	0.19	0.7	$\Gamma_h/\Gamma_e$ $ ^Z$		43
$\lambda'_{133}$	0.55	0.48	0.003	$\nu_e$ -mass	$\tilde{b}$ L-R mixing	42

fermions. The  $\beta\beta 0\nu$  process is a very sensitive probe of  $\mathcal{I}$  interactions in general and of  $\tilde{H}_p$  SUSY in particular as originally discussed in Ref. <sup>29</sup> and further studied in <sup>30</sup>. This is essentially due to the presence in  $\tilde{H}_p$  SUSY of Majorana heavy fermions such as the  $\chi_1^0$  <sup>31</sup>. Besides the  $\chi_1^0$  (or  $\tilde{g}$ ) the  $\beta\beta 0\nu$  involves either the  $\tilde{e}_L$  or the  $\tilde{u}_L$  and  $\tilde{d}_R$ . A detailed investigation taking into account all relevant diagrams <sup>29</sup> as well as the mixing in the gaugino-Higgsino sector was carried in <sup>32</sup>. The transition calculations are performed in the non-relativistic impulse approximation and require a detailed evaluation of the proper nuclear matrix element taking into account short-range correlations.

Using the published result of  $T_{1/2,++}^{\beta\beta 0\nu}({}^{76}\text{Ge}) > 5.6 \times 10^{24}$  years (90% CL) on the half-life of  ${}^{76}\text{Ge}$  published by the Heidelberg-Moscow Collaboration <sup>34</sup>,

stringent limits are deduced on  $\lambda'_{111}$  from the dominant  $\tilde{g}$  exchange contribution. For  $M_{\tilde{u}_L} \simeq M_{\tilde{d}_R}$  and following<sup>32</sup>, we obtain when extrapolating to 95% confidence

$$\lambda'_{111} \lesssim 3.1 \times 10^{-3} (M_{\tilde{g}}/150 \text{ GeV})^2 (M_{\tilde{g}}/1000 \text{ GeV})^{1/2} .$$

Under the hypothesis that  $M_{\tilde{u}_L} \gg M_{\tilde{d}_R}$  or  $M_{\tilde{d}_R} \gg M_{\tilde{u}_L}$ , this slightly weakens to

$$\lambda'_{111} \lesssim 4.5 \times 10^{-4} (M_{\tilde{g}}/150 \text{ GeV})^2 (M_{\tilde{g}}/1000 \text{ GeV})^{1/2} .$$

At large masses the limits deteriorate faster (i.e.  $\propto \tilde{M}^{5/2}$ ) than for other processes (e.g. tests of CC or  $e\text{-}\mu\text{-}\tau$  universality, etc.) involving usual four-fermion operators (i.e.  $\propto \tilde{M}^1$ ). The number in Table 4 is given at  $M_{\tilde{g}} = 1000 \text{ GeV}$  and assuming squark mass degeneracy. It should be noted that the  $\beta\beta\nu$  also severely constrains the coupling combinations  $\lambda'_{11i}, \lambda'_{1i1}$  through diagrams involving the exchange of a  $W$  boson and a mixing of  $f_L$  and  $f_R$  components of scalar bosons (e.g.  $\tilde{q}$ )<sup>35,36</sup>.

Besides constraints from flavour changing neutral currents (FCNC) which are discussed below, the most stringent constraints on  $\lambda'_{112}$  and  $\lambda'_{113}$  comes from their contributions to violation of the universality of lepton and quark couplings to the  $W$  boson in the SM (CC-universality). The presence of one dominant  $\lambda'$  coupling gives extra contributions to quark semileptonic decays as it changes the  $(V - A) \times (V - A)$  structure of the effective four-fermion interaction and affects relative sizes of left-handed mixing angles. Thus a constraint is derived<sup>37</sup> from the comparison of the measured sum of Cabbibo-Kobayashi-Maskawa (CKM) matrix elements  $\sum |V_{udj}|^2$  with SM expectations to which  $\tilde{H}_p$  SUSY adds a positive contribution proportional to  $(\lambda'/M_{\tilde{d}_R}^2)$ . The 95% upper limit in Table 4 is calculated conservatively assuming that the  $\lambda'$  would saturate a deviation at the  $m + 1.64\sigma_m$  level from the measured value  $m$ . The latest experimental value<sup>38</sup> of  $\sum |V_{udj}|^2 = 0.9965 \pm 0.0021$  is used. The limits on  $\lambda'_{11k}$  from CC universality<sup>37</sup> affect only the  $\tilde{d}_R^k$ .

Of course, stringent constraints are also derived from changes induced on (mainly) the longitudinal  $W$  coupling which in turn affects universality in the leptonic sector. The  $e\text{-}\mu\text{-}\tau$  universality has been precisely tested by comparing  $\pi \rightarrow e\nu(\gamma)$  and  $\pi \rightarrow \mu\nu(\gamma)$  decays. The measurement of the ratio  $R_\pi^{exp}/R_\pi^{SM}$  where  $R_\pi = \Gamma(\pi \rightarrow e\nu(\gamma))/\Gamma(\pi \rightarrow \mu\nu(\gamma))$  is thus used<sup>37</sup> to set stringent limits on  $\lambda'_{11k}$  couplings of  $\tilde{d}_R^k$  squarks. The 95% upper limit quoted in Table 4 is derived following<sup>37</sup> and using the most recent measurement<sup>38</sup> value of  $R^{exp} = 1.230(\pm 0.004) \times 10^{-4}$  which is compared with recent theoretical estimates<sup>39</sup> (including radiative corrections).

Semileptonic  $D$  decays extend the  $e$ - $\mu$ - $\tau$  universality constraints to processes involving the second quark generation<sup>40</sup>. Upper limits are derived from the ratios  $R_{D^+}^{e\pi p}$  and  $R_{D^0}^{e\pi p}$  where  $R_D = \Gamma(D \rightarrow K e \nu_e) / \Gamma(D \rightarrow K \mu \nu_\mu)$ , neglecting the virtuality dependence of the hadronic matrix elements involved. The limits quoted in Table 4 were derived in<sup>40</sup> and are here extrapolated to 95% confidence. For the  $D^0$  decays, the latest<sup>38</sup> experimental value of  $(R_D^0)^{-1} = 0.89 \pm 0.07$  as been used.

Upper limits are derived<sup>37</sup> from tests of from Atomic Parity violation using here also the latest experimental input<sup>38</sup>. Constraints from forward-backward asymmetries<sup>37,41</sup> in  $e^+e^-$  collisions are still dominated by experimental errors on axial couplings  $g_a^c$  and  $g_a^b$  of  $b$  and  $c$  quarks (while the uncertainty on  $g_a^c$  has been considerably reduced at LEP).

The presence in  $\mathcal{R}_p$  SUSY of massive scalar bosons possessing  $\mathcal{L}$  couplings is dangerous as they can enter in internal loops giving a mass to the neutrinos. Hence, constraints can be inferred<sup>42</sup> from the upper limits on  $M_{\nu_e}$  which only receives contributions for  $\lambda'_{1jk} \times \lambda'_{1kj}$  coupling products<sup>40</sup> of which  $j = k$  is a special case. From a close inspection of the  $\mathcal{R}_p$  Lagrangian (Eq. 2) it is clear that this contribution depends crucially on the mass mixing between the superpartners  $\tilde{f}_L$  ( $\tilde{f}_R$ ) of the left- (right-)handed fermions  $f_L$  ( $f_R$ ). No  $\lambda'_{1jj}$  limits can be deduced here in absence of squark mass-mixing. The off-diagonal terms in  $\tilde{q}$  mass matrices scale with  $(Am_0 + \mu \tan \beta) \times M_q$  for  $d$ -like squarks where  $A$  and  $m_0$  are SUSY breaking parameters. In Refs.<sup>42,40</sup> it is implicitly assumed that  $Am_0 \gg \mu \tan \beta$ . The same prescription is followed for the upper limits on  $\lambda'_{122}$  and  $\lambda'_{133}$  in Table 4 where we make use of the latest constraint  $M_{\nu_e} \lesssim 15$  eV evaluated by the Particle Data Group<sup>38</sup>. The  $\lambda'_{1jj}$  limits are weaker by a factor up to  $\sim 5$  than those given for a wide possible choice of MSSM parameters (e.g. in the region at  $\mu \ll 0$  with  $\tan \beta = 1$  where the LSP is  $\tilde{\gamma}$ -dominant).

When considering a combination of couplings, a sensitivity comparable to existing indirect LFV limits<sup>28</sup> is obtained by ZEUS<sup>27</sup> at  $M_{\tilde{q}} \simeq 150$  GeV for some coupling combinations.

## 6 Discovery Prospects

In case of a discovery at HERA, the combination of the total cross-section and the branching ratio into  $\mathcal{R}_p$  and gauge decays would uniquely measure the value of the Yukawa coupling  $\lambda'$ . The branching ratio fractions in the various gauge decays would then allow to determine the  $M_2$  and  $\mu$  parameters. This can be seen in Fig. 14. For example, the measurement of the relative branching ratio in  $S3$  and  $S4$  in case of a discovery, could be used to constrain the  $\chi_1^0$

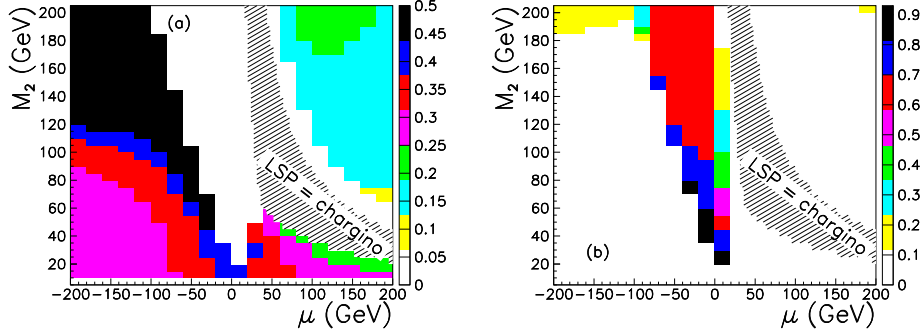


Figure 14: (a) Ratio  $B_{S1}/(B_{S1} + B_{S3})$  of the squark decay branching ratio into the “ $H_p$ ” decay mode  $S1$  and the “gauge” decay mode  $S3$  viewed in the  $M_2$  versus  $\mu$  plane; (b) Similar plot for the ratio  $B_{S4}/(B_{S3} + B_{S4})$  of the squark “gauge” decay branching ratios in channels without  $\cancel{P}_\perp$  involving a like sign ( $S3$ ) and unlike sign ( $S4$ ) lepton. The plots are obtained for  $M_{\tilde{q}} = 150$  GeV at the expected limit of  $\lambda'$  coupling sensitivity for an integrated HERA luminosity of  $100 \text{ pb}^{-1}$ .

LSP nature in the MSSM parameter space as seen in Fig. 14b.

To quantify the future mass-coupling reach of HERA, we derive exclusion limits for the Yukawa couplings  $\lambda'_{1jk}$  as a function of mass in the eventual absence of a significant deviation from the SM expectations. All channels are combined with proper branching ratios and assuming realistic detection efficiencies. The results are shown in Fig. 15 assuming a 40 GeV  $\tilde{\gamma}$ -like  $\chi_1^0$ . The limits are plotted at 95% confidence level (CL), for integrated luminosities of  $L = 100 \text{ pb}^{-1}$  and  $L = 500 \text{ pb}^{-1}$ . For  $L = 500 \text{ pb}^{-1}$ , the existence of first generation squarks with  $H_p$  Yukawa coupling  $\lambda'_{1j1}$  could be excluded for masses up to  $\sim 270$  GeV for coupling strengths  $\lambda_{111}^2/4\pi \gtrsim \alpha_{em}$ .

From the analysis of the  $\lambda'_{1j1}$  case involving the  $\tilde{d}_R$  and  $\tilde{u}_L$  squarks, limits have been deduced on the  $\lambda'_{1jk}$  by folding in the proper parton densities. Such limits are given in Table 5 at  $M_{\tilde{q}} = 150$  GeV and for an eventual integrated luminosity of  $500 \text{ pb}^{-1}$ . The HERA sensitivity to explicit LFV processes at a high integrated luminosity of  $500 \text{ pb}^{-1}$  was studied in <sup>45</sup>. A new range of possible coupling products can be probed for several coupling combinations.

By the time HERA reaches high luminosity running conditions, new direct limits (or a discovery !) from other colliders will have further constrained the possible squark masses and SUSY parameters. It is likely that in  $e^+e^-$  collisions at LEP 200 where squarks are dominantly pair produced through gauge couplings, squarks masses up to near the kinematical limit of  $\sqrt{s_{e^+e^-}}/2 \simeq$

Figure 15: Exclusion upper limits at 95% CL on the  $\lambda'_{1j1}$  coupling as a function of squark mass which could be reached with  $e^+p$  collisions at HERA ( $\sqrt{s} \sim 300$  GeV) for integrated luminosities of  $L = 100 \text{ pb}^{-1}$  (dark shaded area) and  $500 \text{ pb}^{-1}$  (shaded).

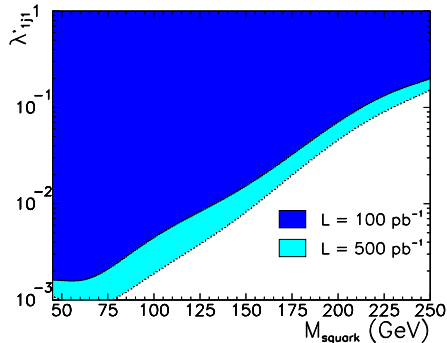


Table 5: Exclusion upper limits at 95% CL on the coupling  $\lambda'_{1jk}$  for  $M_{\tilde{q}} = 150$  GeV and  $M_{\chi_1^0} = 40$  GeV expected for a future integrated luminosity at HERA of  $\mathcal{L} = 500 \text{ pb}^{-1}$ .

Future <b>HERA</b> sensitivity		
	$\tilde{\gamma}$ -like $\chi_1^0$	$\tilde{Z}$ -like $\chi_1^0$
$\lambda'_{111}$	0.008	0.023
$\lambda'_{112}$	0.020	0.057
$\lambda'_{113}$	0.026	0.072
$\lambda'_{121}$	0.008	0.023
$\lambda'_{122}$	0.027	0.077
$\lambda'_{123}$	0.043	0.120
$\lambda'_{131}$	0.007	0.024
$\lambda'_{132}$	0.027	0.091
$\lambda'_{133}$	0.068	0.230

90 GeV can be reached within few years. In  $p\bar{p}$  collisions at the TEVATRON, squarks can be produced in pairs or in association with gluinos. Given the current mass reach for scalar leptoquark and MSSM searches in D0 and CDF experiments, it is likely that  $M_{\tilde{q}} \gtrsim 200$  GeV can be probed through part of the MSSM parameter space even for  $M_{\tilde{g}} > M_{\tilde{q}}$ . Such a mass reach might be provided already by di-lepton data alone as was inferred in ref.<sup>26</sup>. From these and from di-lepton data<sup>26</sup>, one can infer that the range  $200 \rightarrow 300$  GeV of  $\tilde{H}_p$  SUSY squark masses will most probably be not fully excluded by TEVATRON data for an integrated luminosity of  $\sim 100 \text{ pb}^{-1}$ , thus leaving open a discovery window at HERA in the hypothesis  $M_{\tilde{g}} \gg M_{\tilde{q}}$ .

## 7 Conclusion

Squarks of  $R$ -parity violating supersymmetry were searched through direct resonant production via Yukawa couplings  $\lambda'_{jk}$  by the H1 and ZEUS experiments at HERA.

Assuming that one of the  $\lambda'_{jk}$  dominates, three families of event topologies were identified for  $R$ -parity violating and gauge decays of squarks. It was found that squark decays via a  $\lambda'$  coupling into  $l+q$  final states dominate only at largest accessible masses, while elsewhere squarks undergo mainly gauge decays into a quark and a (generally) unstable gaugino-higgsino. No significant evidence for the production of squarks was found in any of the channels and mass dependent limits on the couplings were derived. The existence of first generation squarks with masses up to  $220 \rightarrow 240$  GeV (depending on the MSSM parameter values) are excluded by H1 at 95% confidence level for  $\lambda'_{j1} \gtrsim \sqrt{4\pi\alpha_{em}}$ . These limits extend beyond the current reach at other existing colliders. At  $M_{\tilde{q}} = 150$  GeV, the upper limits obtained for the four couplings  $\lambda'_{jk}$  with  $j \neq 1$  and  $j \neq k$  are comparable or better than the most stringent indirect limits existing.

## Acknowledgments

We wish to thank the organizers of the Workshop and the Chairman Prof. H.V. Klapdor-Kleingrothaus for providing us this opportunity to connect HERA Physics with cosmology and with low energy precision experiments. We are indebted to Dr. H. Dreiner for his collaboration in recent studies on  $R$ -parity violating Supersymmetry at HERA. We thank Dr. G. Bhattacharyya for helpful discussion. We thank our colleagues from the "Search" groups of the H1 and ZEUS Collaborations.

## References

1. For a phenomenological review see for instance  
H.E. Haber and G.L. Kane, Phys. Rep. 117 (1985) 75.
2. For reviews on Supergravity see  
P. Van Nieuwenhuizen, Phys. Rep. 68 (1981) 189 or H.P. Nilles, Phys. Rep. 110 (1984) 1 and references therein.
3. L.J. Hall and M. Suzuki, Nucl. Phys. B231 (1984) 419.
4. S. Dawson, Nucl. Phys. B261 (1985) 297; S. Dimopoulos and L.J. Hall, Phys. Lett. B207 (1987) 210.
5. L.E. Ibáñez and G.G. Ross, Nucl. Phys. B368 (1992) 3.
6. A. Nelson and S. Barr, Phys. Lett. B246 (1990) 141; H. Dreiner and G.G. Ross, Nucl. Phys. B410 (1993) 188.

7. A. Masiero and A. Riotto, Phys. Lett. B289 (1992) 73; U. Sarkar and R. Adhikari, Ahmedabad Phys. Res. Lab, Spires E-preprint hep-ph/9608209.
8. J. Ellis et al., Phys. Lett. B150 (1985) 142; G.G. Ross and J.W.F. Valle, Phys. Lett. B151 (1985) 375; M.C. Bento, L. Hall and G.G. Ross, Nucl. Phys. B292 (1987) 400; D.E. Brahm and L.J. Hall, Phys. Rev. D40 (1989) 2449; S. Lola and G.G. Ross, Phys. Lett. B314 (1993) 336; A.Y. Smirnov and F. Vissani, Nucl. Phys. B460 (1996) 37; *idem*, Phys. Lett. B380 (1996) 317.
9. J. Butterworth and H. Dreiner, Proc. of the Workshop Physics at HERA, W. Buchmüller, G. Ingelman (Editors), DESY Hamburg (October 1991) p1079; *Idem*, Nucl. Phys. B397 (1993) 3.
10. H1 Collaboration, T. Ahmed et al., Z. Phys. C64 (1994) 545.
11. E. Perez and Y. Sirois, Proc. Workshop on Supersymmetry and Unification of Fundamental Interactions, Editions Frontières, I. Antoniadis and H. Videau (Editors), Palaiseau, France (May 1995) p21;
12. H1 Collaboration, S. Aid et al., Z. Phys. C71 (1996) 211.
13. Y. Sirois, Proc. of the 4th Int. Conf. on Supersymmetries in Physics, R. Mohapatra (Editor) College Park, Maryland, USA (May 1996), Spires E-preprint hep-ph/9611457.
14. E. Perez, “Recherche de Particules en Supersymétrie Violant la R-parité dans H1 à HERA”, Thèse de Doctorat, DAPNIA/SPP report 96-1008 (in French).
15. H. Dreiner, P. Morawitz, Nucl. Phys. B428(1994) 31.
16. H1 Collaboration, S. Aid et al., Phys. Lett. B369 (1996) 173.
17. W. Buchmüller, R. Rückl and D. Wyler, Phys. Lett. B191 (1987) 442.
18. J.F. Gunion, H.E. Haber, Nucl. Phys. B272 (1986) 1.
19. A. Bartl, H. Fraas, W. Majerotto and B. Mosslächer, Z. Phys. C55 (1992) 257.
20. H. Dreiner, E. Perez and Y. Sirois Proc. Workshop Future Physics at HERA 1995/96, G. Ingelman et al. (Editors), p. 295.
21. ALEPH Collaboration, D. Buskulic et al., Phys. Lett. B349 (1995) 238.
22. E. Perez, on behalf of H1 and ZEUS Collaborations, to be published in the proceedings of the XXVIIIth International Conference on High Energy Physics, World Scientific (Editor), Warsaw (25-31 July 1996).
23. H1 Collaboration, T. Ahmed et al., DESY preprint 94-248 (December 1994) 9pp.
24. D0 Collaboration, S. Abachi et al., Phys. Rev. Lett. 75 (1995) 618.
25. CDF Collaboration, F. Abe et al., Phys. Rev. Lett. 75 (1995) 613.

26. M. Guchait, D.P. Roy, Phys. Rev. D54 (1996) 3276; H. Dreiner, M. Guchait and D.P. Roy, Phys. Rev. D49 (1994) 3270.
27. ZEUS Collaboration, M. Derrick et al., DESY preprint 96-161 (August 1996) 38pp.
28. S. Davidson, D. Bailey and B.A. Campbell, Z. Phys. C61 (1994) 613.
29. R.N. Mohapatra, Phys. Rev. D34 (1986) 3457.
30. J.D. Vergados, Phys. Lett. B184 (1987) 55; M. Hirsch, H.V. Klapdor-Kleingrothaus and S.G. Kovalenko, Phys. Lett. B352 (1995) 1.
31. R.N. Mohapatra, Proc. Workshop on Neutrinoless Double Beta decay, Trento, Italy (April 1995) 20pp.
32. M. Hirsch, H.V. Klapdor-Kleingrothaus, S.G. Kovalenko, Phys. Rev. Lett. 75 (1995) 17.
33. M. Hirsch, H.V. Klapdor-Kleingrothaus, S.G. Kovalenko, *ibid* Proc. Workshop on Neutrinoless Double Beta decay, Trento, Italy (April 1995) 91-109.
34. Heidelberg-Moscow Collaboration, A. Balysh et al., Phys. Lett. B356 (1995) 450.
35. K.S. Babu and R.N. Mohapatra, Phys. Rev. Lett. 75 (1995) 2276.
36. M. Hirsch, H.V. Klapdor-Kleingrothaus, S.G. Kovalenko, Phys. Lett. B372 (1996) 181; Erratum *ibid* B381 (1996) 488.
37. V. Barger, G.F. Giudice, T. Han, Phys. Rev. D40 (1989) 2987.
38. Particle Data Group, R.M. Barnett et al., Phys. Rev. D54 (1996) 1.
39. W.J. Marciano, Proc. Third Workshop on Tau Lepton Physics, Montreux, Switzerland (September 1994), Nucl. Phys. B (Proc. Suppl.) 40 (1995) 3.
40. G. Bhattacharyya, D. Choudhury, Mod. Phys. Lett. A10 (1995) 1699.
41. G. Bhattacharyya, Proc. 4th International Conference on Supersymmetries in Physics, R. Mohapatra (Editor) College Park, Maryland, USA (May 1996), Spires E-Preprint hep-ph/9608415.
42. R. Godbole, P. Roy, X. Tata, Nucl. Phys. B401 (1993) 67.; S. Dimopoulos, L.J. Hall, Phys. Lett. B207 (1987) 210.
43. G. Bhattacharyya, J. Ellis, K. Sridhar, Mod. Phys. Lett. A10 (1995) 1583.
44. K. Agashe and M. Graesser, Lawrence Berkeley National Laboratory preprint LBL-37823 and University of California preprint UCB-PTH-95/33 (October 1996) 18pp.
45. F. Sciulli and S. Yang, Proc. of the Workshop Future Physics at HERA 1995/96, G. Ingelman et al. (Editors), p. 260.